NeuroImage: Clinical 6 (2014) 475–487

Contents lists available at ScienceDirect

NeuroImage: Clinical

journal homepage: www.elsevier.com/locate/ynicl

Increased cortical curvature reflects white matter atrophy in individual patients with early multiple sclerosis

Michael Deppe[a,*], Jasmin Marinell[a], Julia Krämer[a], Thomas Duning[a], Tobias Ruck[a], Ole J. Simon[a], Frauke Zipp[b], Heinz Wiendl[a], Sven G. Meuth[a]

[a]Department of Neurology, Westfälische Wilhelms University, Münster, Germany
[b]Department of Neurology, Rhine Main Neuroscience Network, Johannes Gutenberg University Medical Centre Mainz, Germany

ARTICLE INFO

Article history:
Received 18 January 2014
Received in revised form 14 February 2014
Accepted 19 February 2014
Available online 3 March 2014

Keywords:
Multiple sclerosis
Imaging
MRI
Cortex
Cortical curvature

ABSTRACT

Objective: White matter atrophy occurs independently of lesions in multiple sclerosis. In contrast to lesion detection, the quantitative assessment of white matter atrophy in individual patients has been regarded as a major challenge. We therefore tested the hypothesis that white matter atrophy (WMA) is present at the very beginning of multiple sclerosis (MS) and in virtually each individual patient. To find a new sensitive and robust marker for WMA we investigated the relationship between cortical surface area, white matter volume (WMV), and whole-brain-surface-averaged rectified cortical extrinsic curvature. Based on geometrical considerations we hypothesized that cortical curvature increases if WMV decreases and the cortical surface area remains constant.

Methods: In total, 95 participants were enrolled: 30 patients with early and advanced relapsing–remitting MS; 30 age-matched control subjects; 30 patients with Alzheimer's disease (AD) and 5 patients with clinically isolated syndrome (CIS).

Results: 29/30 MS and 5/5 CIS patients showed lower WMV than expected from their intracranial volume (average reduction 13.0%, $P < 10^{-10}$), while the cortical surface area showed no significant differences compared with controls. The estimated WMV reductions were correlated with an increase in cortical curvature ($R = 0.62$, $P = 0.000001$). Discriminant analysis revealed that the curvature increase was highly specific for the MS and CIS groups (96.7% correct assignments between MS and control groups) and was significantly correlated with reduction of white matter fractional anisotropy, as determined by diffusion tensor imaging and the Expanded Disability Status Scale. As expected by the predominant gray *and* WM degeneration in AD, no systematic curvature increase was observed in AD.

Conclusion: Whole-brain-averaged cortical extrinsic curvature appears to be a specific and quantitative marker for a *WMV–cortex disproportionality* and allows us to assess "pure" WMA without being confounded by intracranial volume. WMA seems to be a characteristic symptom in *early* MS and can already occur in patients with CIS and should thus be considered in future MS research and clinical studies.

1. Introduction

1.1. Clinical background

Multiple sclerosis is a chronic, multifocal, demyelinating disorder of the CNS with progressive neurodegeneration caused by autoimmune-inflammatory components. MRI characteristics of the disease include multifocal white matter (WM) and gray matter (GM) lesions, brain atrophy, pseudoatrophy, and occult changes in normal-appearing WM and GM (Pirko et al., 2007; Zivadinov, 2007; Zivadinov et al., 2008), highlighting the pathological significance of measures beyond lesion number and volume (Miller et al., 2002). Visualizing and measuring tissue loss in the CNS of patients with multiple sclerosis presents challenges, as it is inevitably easier to capture an image of conspicuous matter, such as in tumor identification, than it is to capture the absence

Abbreviations: 3D, three-dimensional; CI, confidence interval; CIS, clinically isolated syndrome; DTI, diffusion tensor imaging; EDSS, Expanded Disability Status Scale; EVAL, Münster Neuroimaging Evaluation System; eWMV, estimated white matter volume; FA, fractional anisotropy; FOV, field of view; GM, gray matter; GMV, gray matter volume; GRAPPA, generalized autocalibrating partially parallel acquisition; ICV, intracranial volume; ROI, region of interest; SD, standard deviation; TE, echo time; TR, repetition time; TSE, turbo spin-echo; WM, white matter; WMV, white matter volume; ΔWMV, WMV − eWMV.

* Corresponding author at: Department of Neurology, Westfälische Wilhelms University, Albert-Schweitzer-Campus 1, Gebäude A1, 48149 Münster, Germany.
E-mail address: mail@Michael-Deppe.de (M. Deppe).

http://dx.doi.org/10.1016/j.nicl.2014.02.012

of matter due to the disappearance of myelin sheaths, axonal loss, or cell death.

Reduction in brain volume can occur by distinct mechanisms, including inflammatory processes, such as brain oedema, and neurodegenerative events, such as the loss of myelin or axons. There is a vast amount of evidence supporting the hypothesis that pathological changes in WM volume (WMV) may occur by mechanisms that are at least partly independent of overt lesion genesis in early multiple sclerosis (Chard et al., 2002; Filippi et al., 2012). The loss of WM, specifically, is considered to be of high pathophysiological relevance and not an epiphenomenon. Brain atrophy, which can be detected very early in the disease course of multiple sclerosis, is strongly related to disability, but is not well reflected by lesion load when examined in larger cohorts (Calabrese et al., 2007; De et al., 2010; Popescu et al., 2013; Turner et al., 2003).

1.2. Overall hypothesis

With the evolution of more sophisticated imaging techniques, the opportunity exists to identify new, increasingly sensitive measures of tissue loss. Such a novel tissue loss-sensitive biomarker would need to avoid any confounding effects of intracranial volume (ICV), absolute brain size, or absolute CSF volume, and would have to reflect actual microstructural changes of the WM as well as functional deficits of the patients. One concept for such a "new" marker was inspired by an everyday life observation (Fig. 1): that an object with signs of minimal volumetric "atrophy" would have an increased extrinsic (mean) surface curvature if the surface area remains largely constant while the volume is reduced. Thus, it was hypothesized that measuring the extrinsic curvature of the cortex may provide a reliable measure of underlying WM atrophy.

1.3. Why measuring curvature to assess a volume?

The idea here was not to assess any absolute or relative volume. The idea was to assess a potential volumetric *change* of the WM with a single time point MRI. An *initial* (single time point) WMV estimation can principally not be used to ensure (slight) atrophy. By definition, *atrophy* is an *acquired* volume loss, but an initially estimated WMV is not related to any earlier volume. Thus we questioned if we could find a measure that must have changed from a normal value to an obviously (quantitatively) altered value if the WM selectively has shrunk in the past? As a potential candidate, we identified the cortical curvature. However, if the analogy to the apple of Fig. 1 should hold, a number of *prerequisites* must be fulfilled. We have to show that: (i) the WM volume is lower in patients with MS, (ii) the cortical surface *area* is not proportionally altered relative to healthy controls, (iii) the cortical curvature of healthy subjects has less variation than the WMV, and (iv) a volume lower than expected from normal controls is correlated with a higher curvature.

Fig. 1. Representative object (apple) with signs of minimal volumetric "atrophy". The wrinkled skin has an increased *extrinsic* curvature.

1.4. Objective and clinical hypotheses

The objective of the present study was to investigate whether the cortical extrinsic curvature could represent a new, robust, and sensitive biomarker to assess loss of WM brain parenchyma in an early stage of multiple sclerosis.

In this context, we tested the following clinical hypotheses:

- The WM is more affected than suggested by inspecting MRI slices visually, even in patients with clinically isolated syndrome (CIS) or early relapsing–remitting multiple sclerosis.
- Curvature as an atrophy marker is correlated to microstructural alterations of the WM.
- The cortical extrinsic curvature (a geometric measure) is possibly a more sensitive structural marker for selective WM atrophy than WMV itself.

2. Materials and methods

2.1. Structure and concept of the study

To test the prerequisites to establish increased cortical curvature as marker for a volumetric *change* (Section 1.3, i–iv) and to test our clinical hypotheses, we performed a study that was structured into the following analyses.

In *Analysis I*, we estimated WMV and GM volume (GMV) in a cohort of patients with early and advanced relapsing–remitting multiple sclerosis (the multiple sclerosis group), age-matched control subjects (the control group) and patients with expected high atrophy of the WM and GM due to their age and a neurodegenerative condition (the Alzheimer's disease group). We were interested in how the expected WM atrophy of the relatively young patients with multiple sclerosis was quantitatively related to the atrophy observed in the Alzheimer's disease group. We further questioned how the absolute WMVs were related to (and thus confounded by) the individual ICVs. To test the hypothesis that effects seen in the multiple sclerosis group could principally also occur in individuals who are potentially in a "pre-state" of multiple sclerosis, we also included five patients with CIS (*Part I-a*). In *Part I-b* of the study, we examined individual cortical GM measures, i.e. the cortical GMV, cortical thickness, and cortical surface area of all participants.

Analysis II aimed to answer the question whether a potential WM–GM disproportion would correlate with an increased cortical extrinsic curvature as demonstrated by the apple in Fig. 1 (*Part II-a*), and, if so, if this increase would be specific to the patients in the multiple sclerosis group (*Part II-b*), and how age, disease duration, and lesion load would be related to any potential curvature alteration (*Part II-c*). *Analysis III* should reveal if any potential geometric properties of the cortex are associated with intrinsic microstructural alterations of the WM as they can be determined by diffusion tensor imaging (DTI).

Analysis IV should clarify if an increase in the cortical extrinsic curvature has any functional correlate, i.e. is related to the disease progression as expressed by the Expanded Disability Status Scale (EDSS) (*Part IV-a*), and, if so, whether this measure would better correlate with the EDSS than the estimated individual volumetric loss of WM brain

parenchyma (denoted in the following as "ΔWMV") or the individual WM lesion load (*Part IV-b*).

2.2. Subjects

Thirty consecutive patients with early and advanced relapsing–remitting multiple sclerosis (EDSS: range 1–5.5, median 1.5; disease duration: range 14–265 months, median 71.5 months) attending our clinic and diagnosed according to revised McDonald criteria (Polman et al., 2011), were assigned to high-resolution structural and diffusion-weighted MRI at 3 T (age: mean 37.9 years, median 36 years, range 26–56 years, standard deviation [SD] 8.5 years). As control subjects (the control group), 30 age-matched neurologically and psychiatrically healthy volunteers were included in the study (age: mean 38.1 years, median 34.5 years, range 23–69 years, SD 13.3 years, *t*-test: $t = 0.08$, $P > 0.93$). The latter subjects were recruited by announcements in local newspapers. The only selection criterion was age to guarantee equal age distribution between both groups. Additionally, a reference group of 30 randomly selected patients with Alzheimer's disease — a neurodegenerative disease known to *strongly* affect WMV *and* GMV was also included (age: mean 65.6 years, range 46–72 years, SD 6.3 years). Finally, five consecutive patients of our outpatient clinic with CIS, age-matched in relation to the control group (age: mean 35.4 years, range 18–54 years, SD 16.5 years, *t*-test: $t = 0.41$, $P > 0.68$) were also included.

Written informed consent was obtained from all 95 study participants. The participants were also informed that the examination could reveal potentially medically significant findings and given the option to request notification in the event of such findings. The interdisciplinary ethics committee of the University of Münster and the Westphalia-Lippe Chamber of Physicians (Ärztekammer Westfalen-Lippe) approved all examinations.

2.3. MRI

All 95 participants (patients with multiple sclerosis, control subjects, patients with Alzheimer's disease, and patients with CIS) were scanned using the same 3 T Siemens TIM Trio MRI scanner and a 12-channel (matrix) head coil (Siemens AG, Erlangen, Germany) and the same parameters and protocols were applied. Images of the following MRI sequences were obtained: a native isotropic 3D MP-RAGE T1-weighted sequence (field of view [FOV] 256 × 256 mm^2, slice thickness 1.0 mm, matrix 256 × 256, no gap, repetition time [TR] 2000 ms, echo time [TE] 2.52 ms, generalized autocalibrating partially parallel acquisition [GRAPPA] factor 2) and axial diffusion-weighted echo planar imaging for (DTI) (41 slices, FOV 230 × 230 mm^2, slice thickness 3.6 mm, matrix 128 × 128, no gap, slice order interlaced, two averages, TR 7000 ms, TE 104 ms, phase encoding direction: anterior to posterior, 20 gradient directions with $b = 1000$ s/mm^2, 5× $b = 0$ s/mm^2, 2 averages, GRAPPA factor 2).

The following MRI sequences were applied only for the patients with multiple sclerosis to assess lesion load: an axial turbo spin-echo (TSE) FLAIR (44 slices, FOV 250 × 250 mm^2, slice thickness 3.0 mm, matrix 256 × 256, TR 9200 ms, TE 88 ms, no gap, slice order interlaced, TI (inversion time) 2300 ms, flip angle 150°), a sagittal TSE FLAIR (32 slices, FOV 240 × 240 mm^2, slice thickness 3.0 mm, matrix 256 × 256, no gap, slice order interlaced), one 3D MP-RAGE T1-weighted after intravenous gadolinium-DTPA (diethylene triamine penta-acetic acid) 0.1 mmol/kg injection, an axial T2-weighted TSE "short" (46 slices, FOV 250 × 250 mm^2, slice thickness 3.0 mm, matrix 256 × 256, TR 4000 ms, TE 18 ms, no gap, slice order interlaced), an axial T2-weighted TSE "long" (46 slices, FOV 250 × 250 mm^2, slice thickness 3.0 mm, matrix 256 × 256, TR 3000 ms, TE 72 ms, no gap, slice order interlaced, GRAPPA factor 2), and an axial proton density-weighted TSE (46 slices, FOV 250 × 250 mm^2, slice thickness 3.0 mm, matrix 256 × 256, TR 3000 ms, TE 17 ms, no gap, slice order interlaced). Head motion was minimized by foam padding.

2.4. DTI data post-processing

All diffusion-weighted images were effectively corrected for eddy currents and head movements using a recently developed algorithm (Mohammadi et al., 2010) and a multi-contrast image registration algorithm for the optimum spatial pre-processing of DTI data (Mohammadi et al., 2012). The registration algorithm provided rigorous iterative multi-contrast registration steps based on FA contrasts and *b*0 contrasts ($b = 0$ s/mm^2), so that volumetric effects in the resulting normalized FA maps were negligible (Mohammadi et al., 2012). All registered diffusivity images corresponded to the MNI (Montreal Neurologic Institute) coordinate space. For quantitative analysis of the optimally spatially registered images, we generated two regions of interest (ROI): one for the whole WM and the other for the corpus callosum. These ROIs that were automatically created on the output images had been employed and validated in earlier studies (Deppe et al., 2007; Kleffner et al., 2008; Wersching et al., 2010). All DTI image-processing steps (registration, eddy current correction, tensor estimation, diffusion parameter, and ROI calculation) were performed in a fully automated (and thus objective) processing pipeline for quantitative assessment of DTI data ("Münster Neuroimaging Evaluation System" [EVAL]) (Deppe et al., 2007, 2008, 2013).

2.5. Individual cortical curvature, thickness, and area analysis

All 3D MP-RAGE images were also transferred to the EVAL and were corrected for lack of homogeneity in intensity using in-house software. All images were automatically processed by software scripts in exactly the same way on an Apple® Mac Pro (OS X 10.7, 32 GB, 2 × 2.93 GHz 6-Core Intel Xeon, Apple® Inc., Cupertino, CA, USA) running FreeSurfer software (Version 5.1; http://surfer.nmr.mgh.harvard.edu/). For details of this method see Dale et al. (1999), Fischl (2012), Fischl and Dale (2000) and Fischl et al. (1999). Briefly, cerebral WM was initially segmented, divided into two hemispheres, and the brainstem and cerebellum were removed. A triangle-based mesh of the WM surface is produced through tessellation, which is subsequently deformed outward to generate the pial surface before automatic correction of topological defects in the resulting main fold. Cortical thickness mean and Gaussian intrinsic curvature measurements were obtained at each vertex by reconstructing representations of the GM–WM boundary and the pial surface. The entire cortex of each patient and control was visually inspected, but no *relevant* errors in cortical labeling could be detected that had to be manually corrected. Thus the whole quantitative brain analysis was completely objective and could not be biased by any subjective factor. Local cortical thickness, rectified extrinsic and Gaussian curvature had been averaged over both cerebral hemispheres using software tools incorporated into FreeSurfer software for each examined individual. Additionally, we calculated the individual total cortical surface area. From the segmented data, we used the cortical WMV and the cortex volume as calculated by FreeSurfer. By summarizing the volumes of WM hypointensities as detected by FreeSurfer in the 3D T1w images we assessed the individual WM "lesion load".

2.6. Group analysis

For the group analyses of all estimated end points, methods based on the Generalized Linear Model (*t*-test, ANOVA, ANCOVA) and discriminant function analysis as provided by the software STATISTICA Version 10 (2011; Stat Soft. Inc., Tulsa, OK, USA) were employed. All reported significant results survived criteria for multiple comparisons.

3. Results

3.1. (Analysis I-a) Patients with multiple sclerosis show WM atrophy comparable to the elderly patients with Alzheimer's disease

An ANOVA (dependent variable WMV, factors: group [control, multiple sclerosis, Alzheimer's disease group] and gender [female, male]) revealed significant main effects for group and gender; [group: $F(2, 84) = 7.1$, $P = 0.0014$; gender: $F(1, 84) = 15.4$, $P = 0.00017$]. No significant group × gender interaction could be observed [$F(2, 84) = 1.7$, $P = 0.18$]. The five CIS patients were not included in the analysis. Post-hoc *t*-tests revealed that the multiple sclerosis patients showed a 13.0% WMV reduction in relation to the control group (multiple sclerosis: mean WMV = 456,303 mm^3, SD 63,116 mm^3; control: WMV = 524,329 mm^3, SD 68,318 mm^3; $P < 0.0002$). The WMV reduction was comparable to the volume reduction of 15.6% seen in the older group of patients with Alzheimer's disease (WMV = 442,631 mm^3, SD 59,574 mm^3; $P < 0.00001$). No significant differences in WMV could be found between the multiple sclerosis and Alzheimer's disease groups, and between the multiple sclerosis and CIS groups. The results are illustrated in Fig. 2 and summarized in Table 1.

WMV was strongly correlated with ICV in the control group ($R = 0.876$; $P < 0.0000001$; control WMV = $-61{,}420$ mm^3 + 0.3881 × control ICV), so that 77% of the WMV variance could be explained by the ICV in the control group (Fig. 3). We used the "control WMV" as the ICV-dependent predictor for the expected WMV (eWMV) in the multiple sclerosis group:

$$\text{eWMV} = -61{,}420\ mm^3 + 0.3881 \times \text{multiple sclerosis ICV}. \quad (1)$$

The difference between "actual multiple sclerosis WMV" in each individual patient and eWMV was calculated as:

$$\Delta\text{WMV} = \text{actual multiple sclerosis WMV} - \text{eWMV}. \quad (2)$$

The arrow in Fig. 3 illustrates the ΔWMV of one patient. The multiple sclerosis patients showed a highly significant negative ΔWMV compared with the control subjects (mean multiple sclerosis ΔWMV = −56,417 mm^3, SD = 43,267 mm^3, $t = -5.68$; $P < 0.000001$). Although the number of CIS patients was very low, and thus also the power of the *t*-test, the CIS patients also showed a significant negative ΔWMV compared with the control subjects (mean CIS ΔWMV = −49,188 mm^3, SD = 18,048 mm^3, $t = -3.23$; $P < 0.003$). The ΔWMV of the control group was about 0 mm^3 because the regression function was estimated by this group. No indication of a systematic difference in ICV between the control and multiple sclerosis groups could be found (multiple sclerosis: 1.48 l, SD = 0.13 l, control: 1.51 l, SD = 0.15 l $t = 0.82$; $P > 0.42$). The same was true for the patients with Alzheimer's disease (1.48 l, SD = 0.14 l, $t = 0.66$; $P > 0.51$).

3.2. (Analysis I-b) Multiple sclerosis patients and controls showed no significant or relevant differences in cortical surface area

An ANCOVA (dependent variable: cortex volume, categorical factors: gender [female, male] and group [control, multiple sclerosis, Alzheimer's disease], continuous factor: age) showed a significant gender effect [$F(1, 83) = 16.66$, $P = 0.0001$], group effect [$F(2, 83) = 3.80$, $P < 0.05$], and age effect [$F(1, 83) = 12.78$, $P < 0.001$], but no group × gender effect [$F(2, 83) = 0.28$, $P = 0.76$]. A post-hoc analysis showed that the cortical volumes differed significantly (7.17%) between the control and multiple sclerosis groups (multiple sclerosis: mean cortex volume = 480,723 mm^3, control: mean cortex volume = 517,863 mm^3, $P < 0.05$). The patients with Alzheimer's disease showed a highly significant (22.87%) decrease in cortical volume (mean cortex volume = 399,414 mm^3; $P < 10^{-9}$).

An ANCOVA (dependent variable: cortical thickness, categorical factors: gender [male, female] and group [control, multiple sclerosis, Alzheimer's disease], continuous factor: age) revealed that age and group had a highly significant main effect on cortical thickness [age: $F(2, 83) = 16.8$; $P < 0.000001$; group: $F(2, 83) = 14.6$; $P < 0.000001$].

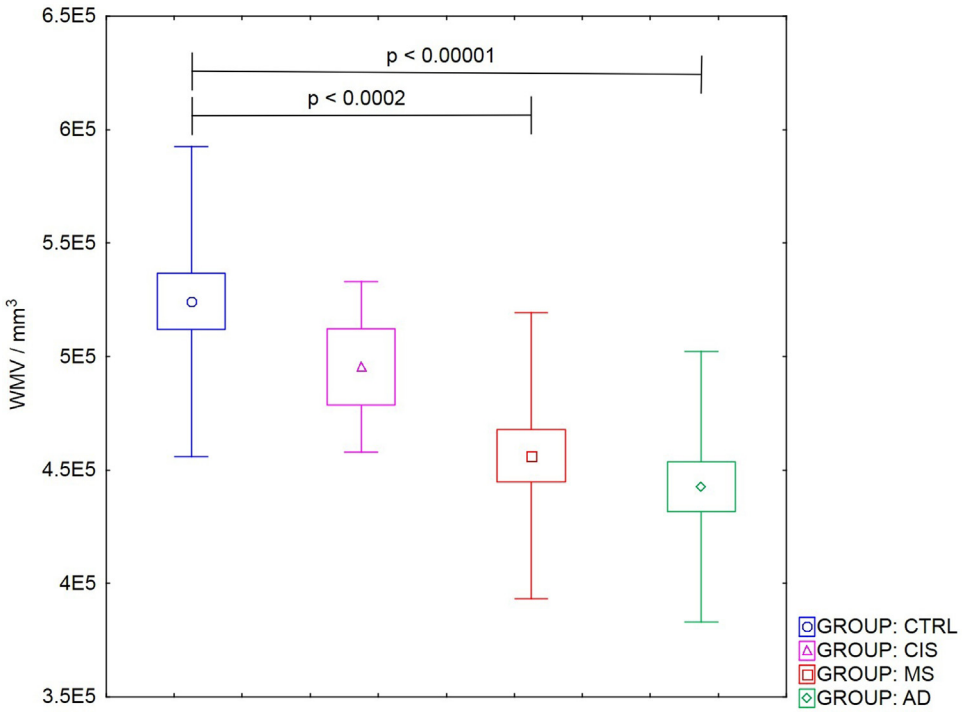

Fig. 2. White matter volumes. Group mean values and significance levels as reported by ANOVA (dependent variable WMV, factors: group and gender). The patients with multiple sclerosis (MS) showed a relevant (13.0%) WM atrophy, that is comparable to that of (much older) patients with Alzheimer's disease (AD). Vertical bars denote the SD and the box the 95% CI of the mean. CTRL = control.

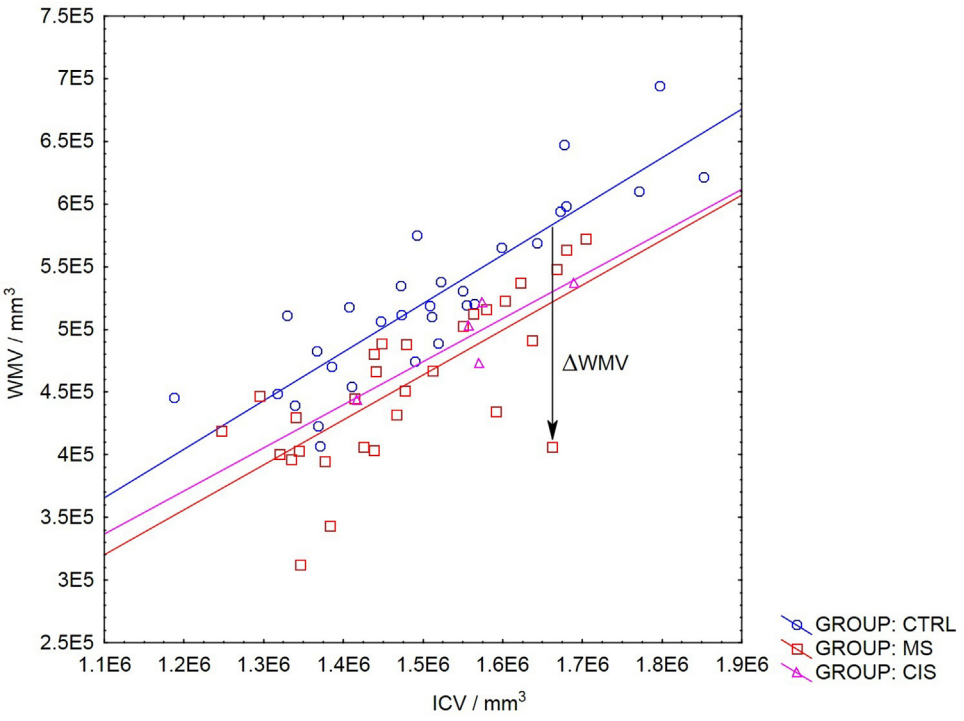

Fig. 3. The WMV was strongly correlated with the ICV in both the multiple sclerosis (MS) and control groups (CTRL). Nearly every multiple sclerosis patient (29/30) showed a lower WMV (= negative "ΔWMV", see arrow) as expected from the relationship between the WMV and ICV of the control group (blue line). The five patients with CIS also had a systematically lower WMV, as expected from their ICV. For details, see text.

We could not observe any gender or group × gender effect on cortical thickness [gender: $F(1, 83) = 0.0014$, $P = 0.97$; group × gender: $F(2, 83) = 0.24$, $P = 0.78$]. The multiple sclerosis patients showed a 3.6% reduction in cortical thickness relative to the control group, while the thickness was reduced by 10.4% in the patients with Alzheimer's disease (multiple sclerosis: mean thickness = 2.42, 95% confidence interval [CI; 2.38, 2.46]; control: mean thickness = 2.51, 95% CI [2.48, 2.55], Alzheimer's disease: mean thickness = 2.23, 95% CI [2.19, 2.27]). The latter results are illustrated in Fig. 4.

An ANOVA (dependent variable: cortical surface area, two factors: group [control, multiple sclerosis, Alzheimer's disease] and, gender [female, male]) revealed a significant group main effect [$F(2, 84) =$

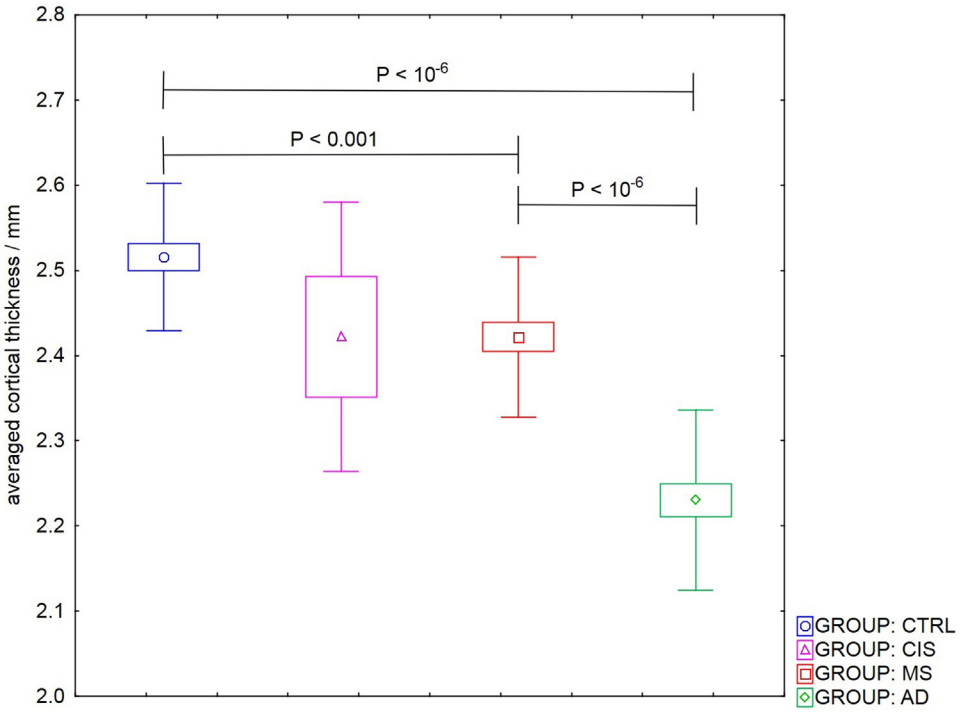

Fig. 4. Cortical thickness. Boxes denote the standard error of the mean and vertical bars the SD of cortical thickness. The multiple sclerosis (MS) patients showed a 3.6% reduction in cortical thickness relative to the control group (CTRL), while the thickness was reduced by 10.4% in the patients with Alzheimer's disease (AD).

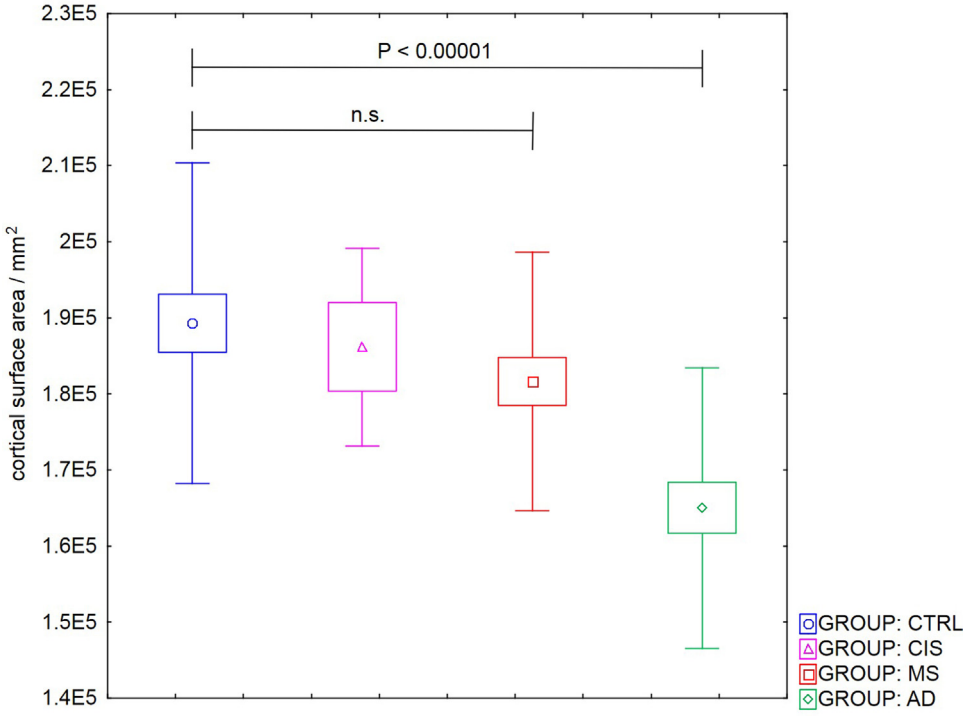

Fig. 5. Cortical surface area. Multiple sclerosis (MS) patients showed no significant (4%) decrease in cortical surface area compared with normal control subjects (CRTL) in contrast to the group of patients with Alzheimer's disease (AD; 12.8%).

11.442, $P = 0.00004$] and a significant gender main effect [$F(1, 84) = 31.199$, $P < 0.000001$], but no significant group × gender effect [$F(2, 84) = 1.46$, $P = 0.24$]. Post-hoc t-tests showed that the group main effect could be attributed to the Alzheimer's disease group (see Fig. 5). The multiple sclerosis patients showed no significant (4%) decrease in cortical surface area compared with the normal control subjects (multiple sclerosis: mean area = 181,652 mm^2, SD = 17,011 mm^2; control: mean area = 189,309 mm^2, SD = 21,104 mm^2, $t = 0.55$, not significant). The group of patients with Alzheimer's disease showed a highly significant 12.8% reduction in cortical surface area (mean area = 165,006 mm^2, SD = 18,408 mm^2; $P < 0.0001$).

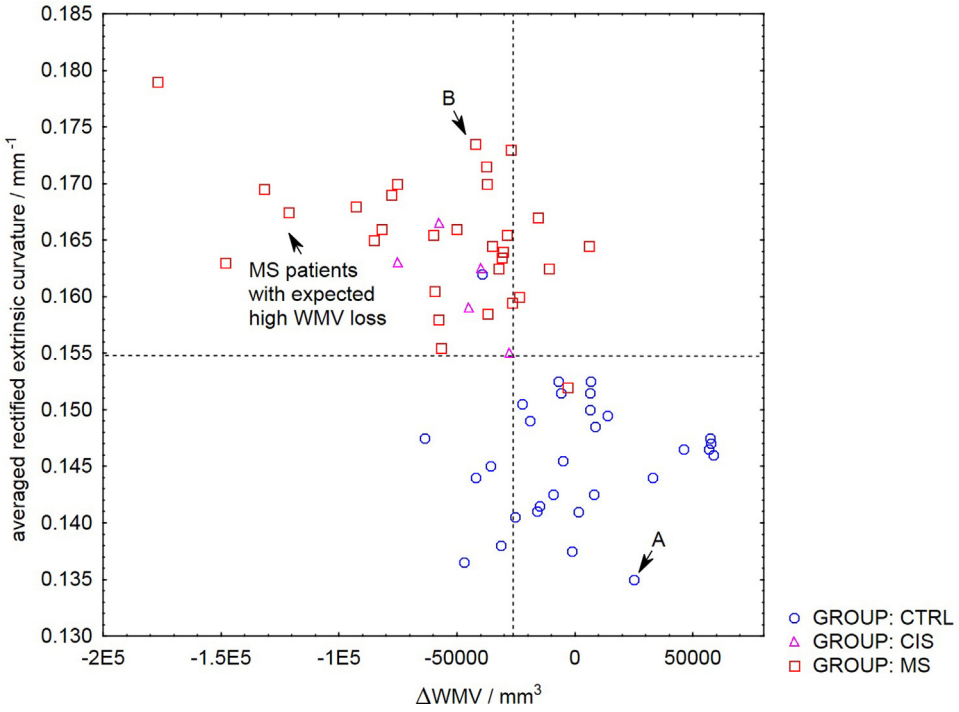

Fig. 6. Integrated cortical extrinsic curvature increases with estimated WMV loss (ΔWMV) in multiple sclerosis patients. Patients with a relatively high estimated WMV loss showed the highest cortical curvature (left arrow). The dashed lines have been calculated by discriminant function analysis to assess the classification power of ΔWMV and extrinsic curvature. For details see text. The letters depict the example control (CTRL) subject ("A") and the multiple sclerosis (MS) patient ("B") referred to in Fig. 8.

3.3. (Analysis II-a) The WM–GM disproportion leads to increased cortical curvature in patients with multiple sclerosis

An overall linear regression between cortical extrinsic curvature and ΔWMV of the multiple sclerosis and control groups revealed a strong relationship between individual cortical extrinsic curvature and eWMV loss: ΔWMV ($R = 0.62$, $P = 0.000001$). Although the ΔWMV and cortical extrinsic curvature were strongly correlated, the results of a discriminant function analysis qualified the extrinsic curvature as the better predictor of classification into the control and multiple sclerosis groups (grand class means for classification: ΔWMV = −26,091 mm^3, 83.3% correct classifications, cortical extrinsic curvature = 0.1548 mm^{-1}, 93.7% correct classifications) (see Fig. 6). Patients with a relatively high eWMV loss showed the highest cortical curvature (linear regression within the multiple sclerosis group: $R = 0.44$, $P = 0.01$). No correlation was found by a group-wise regression analysis within the control group ($R = 0.033$, $P = 0.86$).

3.4. (Analysis II-b) The individually increased cortical extrinsic curvature seems to be specific to a WM–GM disproportion

The ANCOVA with dependent variable cortical extrinsic curvature and categorical factors gender [female, male], group [multiple sclerosis, control, Alzheimer's disease], and continuous predictor age revealed that the factor group had the largest main effect on the cortical curvature [$F(2, 83) = 40.0$; $P < 0.0000001$], age produced no significant effect ($F = 0.3$; $P > 0.60$), while the curvature is slightly influenced by gender [$F(1, 83) = 12.1$; $P < 0.001$], but no group-specific gender effect could be observed [gender × group effect: $F(2, 83) = 1.3$, $P = 0.27$]. Post-hoc *t*-tests demonstrated that the multiple sclerosis patients showed a highly significant 13.3% increase in cortical curvature in relation to the age-matched control group (multiple sclerosis: extrinsic curvature = 0.165 mm^{-1}, SD 0.0057 mm^{-1}; control: extrinsic curvature = 0.146 mm^{-1}, SD 0.0057 mm^{-1}, $P < 10^{-10}$). The CIS group also showed a significantly increased cortical extrinsic curvature (CIS: extrinsic curvature = 0.161 mm^{-1}, SD 0.0044 mm^{-1}, $P < 0.0001$). The group of patients with Alzheimer's disease showed no change in cortical curvature in relation to the control group (Alzheimer's disease: extrinsic curvature = 0.145 mm^{-1}, SD 0.0128 mm^{-1}, $P = 0.88$). These results are summarized in Fig. 7.

A representative example subject from each of the three groups (control, multiple sclerosis, and Alzheimer's disease) is shown in Fig. 8 to illustrate how the mathematically abstract value of *rectified extrinsic curvature* is associated with the individual appearance of sulci and gyri in corresponding T1-weighted MRI slices. Fig. 9 illustrates how the local extrinsic curvature was determined for the same control subject and multiple sclerosis patient shown in Fig. 8 by FreeSurfer software.

3.5. (Analysis II-c) Impact of disease duration, age, lesion load, and ICV on cortical extrinsic curvature

Neither the multiple sclerosis nor the control group showed a significant impact of age on cortical extrinsic curvature. In addition, the disease duration had no significant impact on the curvature. Additionally, already the 4 CIS and 5 RRMS patients with a disease duration of less than 24 months showed curvatures above the values of nearly all normal controls. The results are illustrated as a scatterplot in Fig. 10. In contrast to the WMV, the whole-brain-averaged cortical extrinsic curvature showed virtually no ICV dependence in the control group ($R = 0.096$, $P = 0.62$). A linear regression with dependent variable cortical extrinsic curvature and factor lesion load showed a weak positive correlation between curvature and lesion load in the group of patients with multiple sclerosis ($R = 0.33$, $P = 0.07$).

3.6. (Analysis III-a) Microstructural correlate within the WMV of increased cortical extrinsic curvature

The mean FA values of the corpus callosum ROI were significantly reduced in the multiple sclerosis group compared with the control group (multiple sclerosis: mean FA 0.365, SD 0.0618; CIS: mean FA 0.398, SD 0.031; control: mean FA 0.420, SD 0.0397, $t = 4.11$, $P < 0.0002$). A linear regression analysis of the mean FA within the

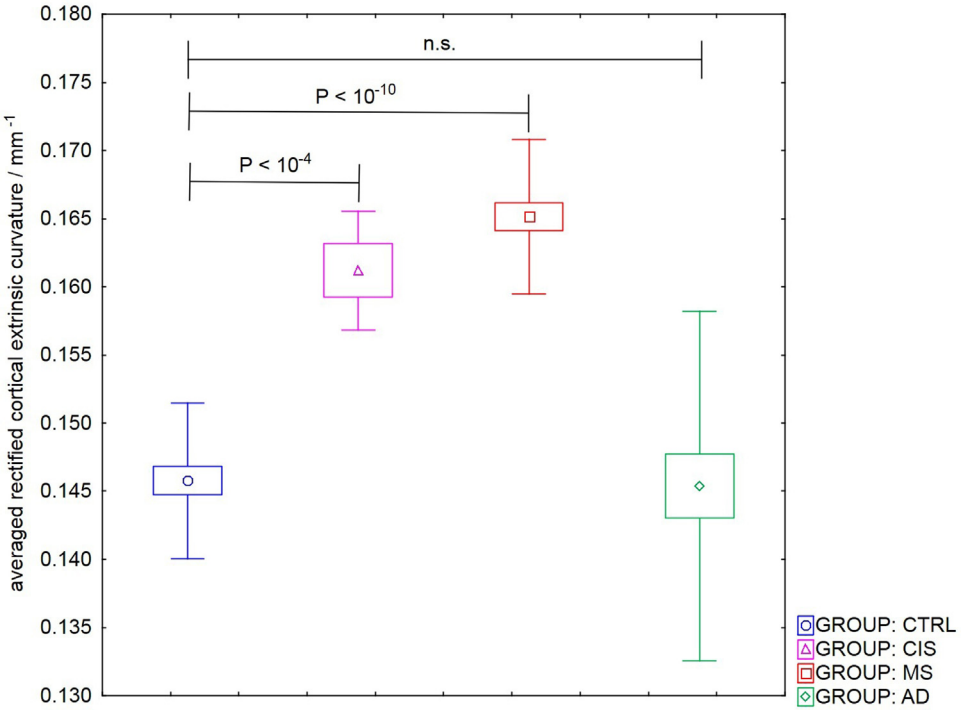

Fig. 7. Cortical extrinsic curvature. The multiple sclerosis (MS) patients showed on average a highly significant 13.3% increase in cortical extrinsic curvature in relation to the age-matched control (CTRL) group. The CIS group also showed a significantly increased cortical extrinsic curvature. Vertical bars denote SDs and boxes standard errors.

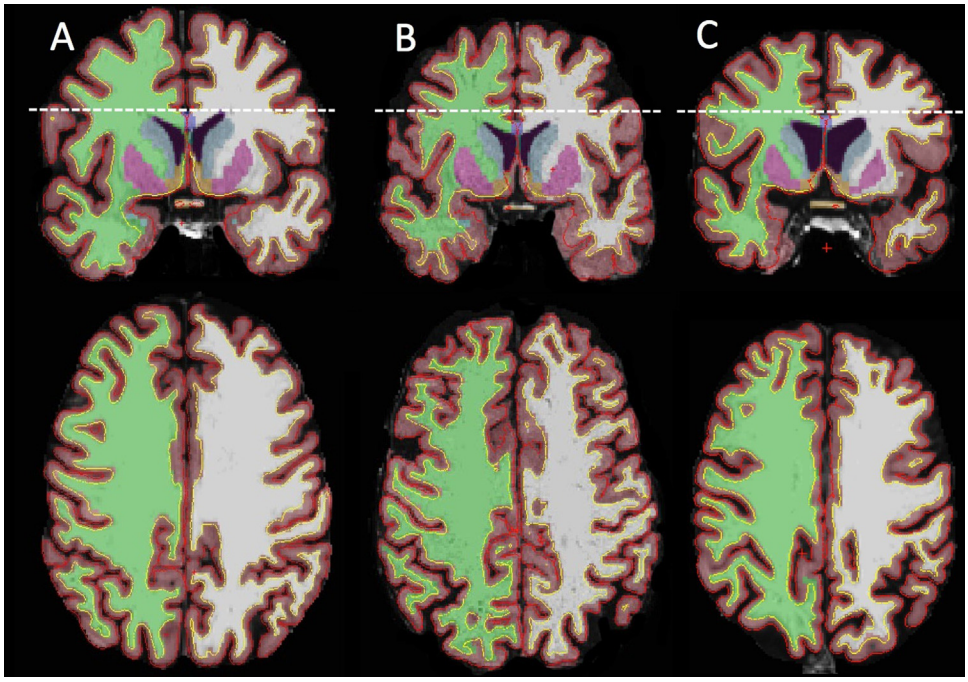

Fig. 8. Illustration of the increased cortical curvature in a patient with multiple sclerosis and quantified WM atrophy relative to a control subject and a patient with Alzheimer's disease. Shown are coronal and sagittal sections of a healthy control subject (A), a patient with multiple sclerosis (B), and a patient with Alzheimer's disease (C). The T1-weighted MRIs are superimposed by structural labels of cortical surfaces (yellow, red), WM (green, white) and cortex (brown) as generated by FreeSurfer software. The mean rectified curvatures of the left (green) and right (white) hemispheres were 0.135 mm^{-1} (left hemisphere [lh])/0.135 mm^{-1} (right hemisphere [rh]) for the control subject and 0.179 mm^{-1} (lh)/0.168 mm^{-1} (rh) for the patient with multiple sclerosis. Cortical WMV was about 15% less in the multiple sclerosis patient relative to the control subject (control: 266,960 mm^3 [lh], 267,879 mm^3 [rh]; multiple sclerosis: 219,878 mm^3 [lh], 225,045 mm^3 [rh]) and about 33% less in the patient with Alzheimer's disease (181,802 mm^3 [lh], 179,325 mm^3 [rh]). By comparing A and B, the increased curvature (>24%) and the WM atrophy can be clearly seen in the patient with multiple sclerosis, while the patient with Alzheimer's disease has obvious WM atrophy, but the cortical curvature looks not only similar to that of the control subject, but is also quantitatively very close to the control subject (0.139 mm^{-1} [lh]/0.138 mm^{-1} [rh]). The average cortical thicknesses showed no relevant (<2%) differences between the control subject, the multiple sclerosis patient, and the patient with Alzheimer's disease (control: 2.344 mm [lh], 2.357 mm [rh]; multiple sclerosis: 2.314 mm [lh], 2.338 mm [rh]; Alzheimer: 2.391 mm [lh], 2.357 mm [rh]). In addition, the total surface areas of the hemispheres of the control subject and the multiple sclerosis patient showed no relevant (<2%) differences (control: 87,562 mm^2 [lh], 87,565 mm^2 [rh]; multiple sclerosis: 86,202 mm^2 [lh], 89,116 mm^2 [rh]). In contrast to the multiple sclerosis patient, the patient with Alzheimer's disease has an about 20% smaller cortical surface relative to the control subject (70,957 mm^2 [lh], 70,029 mm^2 [rh]).

ROI of the corpus callosum revealed that the increase in the cortical curvature in patients with multiple sclerosis was significantly correlated with the WM integrity loss as assessed by FA ("extrinsic curvature" $= 0.178\ mm^{-1} - 5.0 \times 10^{-2}\ mm^{-1} \times$ "FA in corpus callosum", $R = 0.50$, $P = 0.006$). For details see Fig. 11.

3.7. (Analysis III-b) Sensitivity and specificity

The two end points "WM integrity loss as assessed by FA" and "averaged cortical extrinsic curvature" allowed a highly specific classification of the 60 examined age-matched subjects into the control and multiple sclerosis groups (Fig. 12). The patients of the Alzheimer's disease group showed predominantly low cortical extrinsic curvature, like the control subjects, but significantly reduced FA (mean Alzheimer's disease: 0.318, mean control: 0.361, $t = -7.33$; $P < 0.000000001$). Interestingly, the 68% probability ellipses of the patients with CIS strongly overlapped with the multiple sclerosis group, but not with the ellipse of the control group.

3.8. (Analysis IV-a) Does WMV atrophy as expressed by the cortical extrinsic curvature have a functional correlate?

A linear regression analysis (Fig. 13) between the EDSS and cortical extrinsic curvature showed that the disease progression of multiple sclerosis, as assessed by the EDSS, is related to an increased cortical extrinsic curvature (linear regression analysis: dependent factor: EDSS, independent factor: cortical curvature, $R = 0.38$, $P = 0.05$). It should be noted here that the EDSS represents a rank ordering of observations (ordinal) rather than a precise measurement of an actual continuous variable. However, the EDSS was assessed in half-steps so that its variability can be considered as *quasi-continuous*.

3.9. (Analysis IV-b) Which measure better predicts disability: estimated volumetric loss of WM brain parenchyma (ΔWMV), cortical thickness, lesion load, or curvature increase?

Cortical extrinsic curvature increase seemed to be a better predictor of functional deficits than the estimated ΔWMV, i.e. correlated significantly with the EDSS in contrast to the ΔWMV (linear regression with dependent variable: EDSS, factor: ΔWMV, $R = 0.30$, $P = 0.10$). Also the WM lesion load and the gray matter volume did not correlate significantly with the EDSS (linear regression with dependent variable: EDSS, factor: lesion load, $R = 0.27$, $P = 0.12$, factor gray matter volume, $R = 0.04$, $P = 0.82$). In addition, individual average cortical thickness of the patients with multiple sclerosis was also not a better predictor of the EDSS than the cortical extrinsic curvature (linear regression dependent variable EDSS, factor cortical thickness $R = 0.16$, $P = 0.40$).

4. Discussion

4.1. Increased cortical extrinsic curvature and WMV loss

The main finding of the present study is that increased cortical extrinsic curvature was observed in patients with multiple sclerosis compared with control subjects and patients with Alzheimer's disease. Most notably, an increased cortical curvature was even shown in patients with CIS, a potentially early sign of multiple sclerosis. It is hypothesized that the curvature increase was most likely caused by WM atrophy in each individual subject (Figs. 3, 6, and 10) and arose

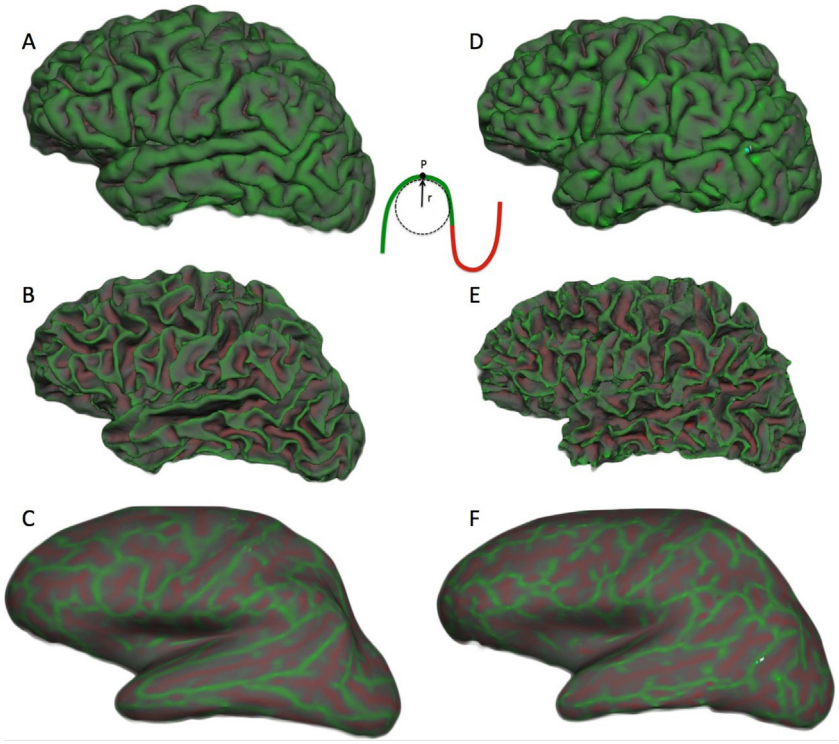

Fig. 9. Illustration of the estimated local cortical extrinsic curvature in the sample control subject (A–C) and the sample patient with multiple sclerosis (D–F) of Fig. 8. Shown are slightly smoothed local extrinsic curvatures of the cortex (pial surface) (A, D) and WM surface (B, E). Negative regions are folded-out and shown in green (gyral), and positive regions are folded-in and shown in red (sulcal). In this study, we only considered the "folding" or extrinsic (mean) curvature, which is defined at every point P on the surface (for details see text books). At each point P, the extrinsic curvature of a plane curve can be illustrated as the inverse of the radius *r* of the *osculating circle*, a circle with a certain tangency and curvature so that it best fits the curve in a certain point P (curvature = 1 / *r*). The WM surface of the multiple sclerosis patient (E) looked obviously "shrunken" with sharper edges at the outer gyri when compared with the WM surface of the control subject (B) with normal WMV.

due to an imbalance of cortex surface area and WMV. A mean WMV reduction of 13.0% was seen in the multiple sclerosis group, with 29/30 patients showing a negative ΔWMV; in contrast, there were no relevant differences seen in cortical volume or surface area between the patients with multiple sclerosis and the control group (Figs. 4 and 5).

The increased cortical extrinsic curvature in the multiple sclerosis group is not an abstract mathematical expression from differential geometry, but can actually be seen in MRI slices when compared with subjects with an average curvature (Fig. 8A, B). The WM shrinkage is also visible, if 3D reconstructed WM surfaces are compared (Fig. 9) (see also Voets et al., 2011). An increased cortical extrinsic curvature seems to be specific to primary WMV loss and a *nearly* (but not fully) intact cerebral cortex. In patients with neurodegenerative Alzheimer's disease, it can be assumed that because of the disease and the age of these patients, the cortex *and* WM were degenerated. There was no systematic disproportion of WMV and cortical GM surface, and, thus, no systematic change in the cortical curvature (Fig. 7). This finding further supports the hypothesis that the WM–GM disproportion is causative of the increased extrinsic curvature.

4.2. Estimation of reduced WMV by ΔWMV

The WMV loss in our study was assessed by an *apparent peculiar* new measure, i.e. ΔWMV. The rationale in favor of this method and against ICV-normalized WM volume or WM fraction was, that ΔWMV is obviously not confounded by whole brain/GM atrophy. A second reason was that ΔWMV allowed easily assessing the absolute volume difference compared to the expectation value of normal controls, i.e. a

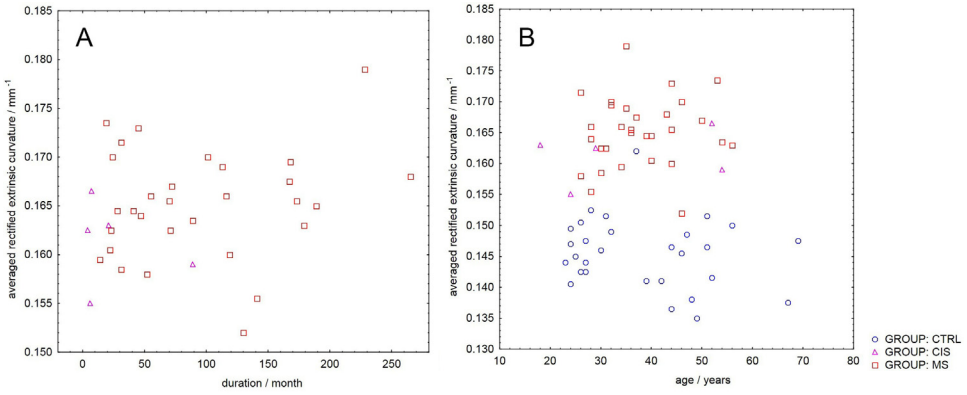

Fig. 10. Cortical mean curvature related to disease duration (A) and age (B). No significant impact of disease duration or age could be observed on cortical extrinsic curvature. MS = multiple sclerosis; CTRL = control.

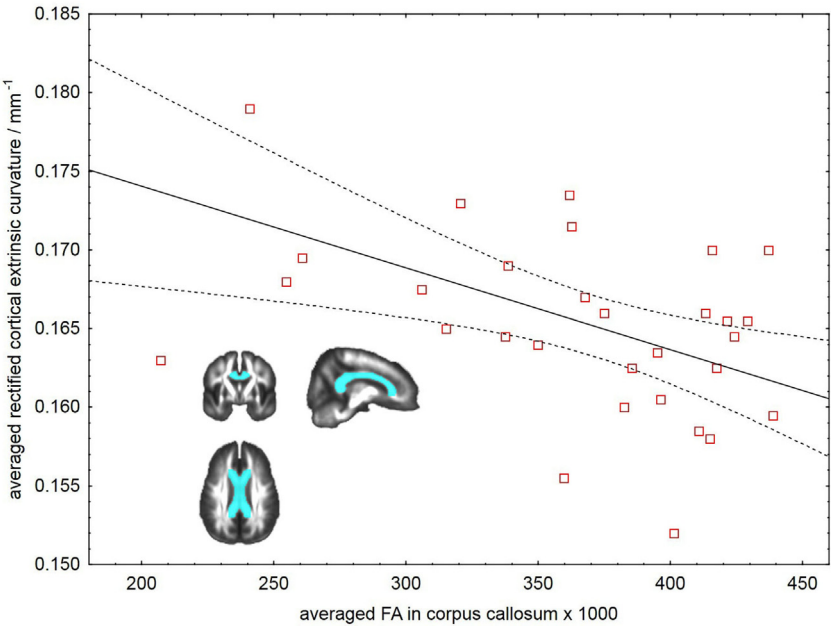

Fig. 11. Reduction of FA in the corpus callosum was significantly correlated with the increase in cortical curvature in multiple sclerosis patients. The three orthogonal brain sections illustrate the ROI employed for averaging the FA of the corpus callosum. Note: the patient with the strongest FA reduction (FA close to 0.200) was regarded as an outlier and excluded from the estimation of the regression function, because the total GMV of this patient (female, 56 years, disease duration 179 month, relapsing–remitting multiple sclerosis) was also extremely and untypically reduced relative to the other multiple sclerosis patients (19% reduction, $P < 0.05$), the WM lesion volume was 400% increased relative to the mean of the other multiple sclerosis patients ($P < 0.00005$) and the cortical WMV was reduced by 33.5% ($P < 0.01$) relative to the other multiple sclerosis patients.

negative value makes immediately clear that the volume is XY mm^3 below the normal average. The calculation of an expectation value for normal WMV was possible due to the strong linear relation between ICV and WMV in healthy controls (Fig. 3). However, it should be noted here, that a negative ΔWMV does not automatically mean that the WM is atrophic. Fifty percent of the healthy subjects have per definition a negative ΔWMV.

4.3. Volume loss and microstructure

To investigate how increased extrinsic curvature is related to potential microstructural alterations of the WM, we employed DTI to assess microstructural tissue damage in normal-appearing WM (Deppe et al., 2008; Duning et al., 2010; Keller et al., 2013). For this purpose, we calculated the FA within a ROI outlining the corpus callosum. The corpus

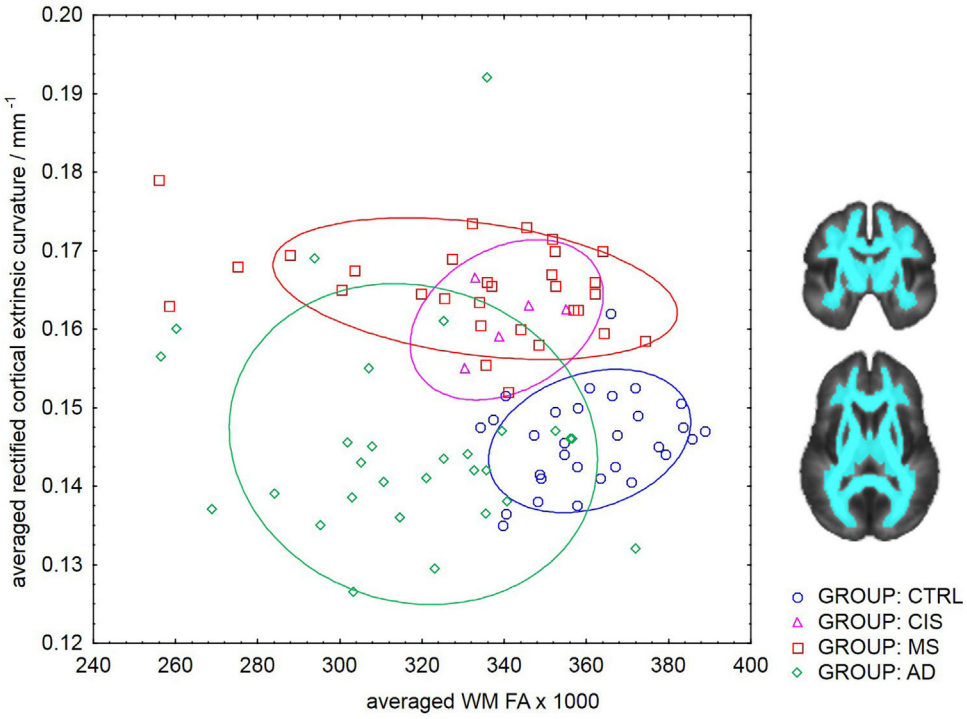

Fig. 12. Cortical curvature in relation to microstructural WM integrity as assessed by FA. The overall microstructural WM integrity was assessed by the mean FA of a whole WM ROI (see brain sections). The ellipses represent the areas of 68% probability to find a subject of the corresponding group ("two-dimensional SD"). AD = Alzheimer's disease; CTRL = control; MS = multiple sclerosis.

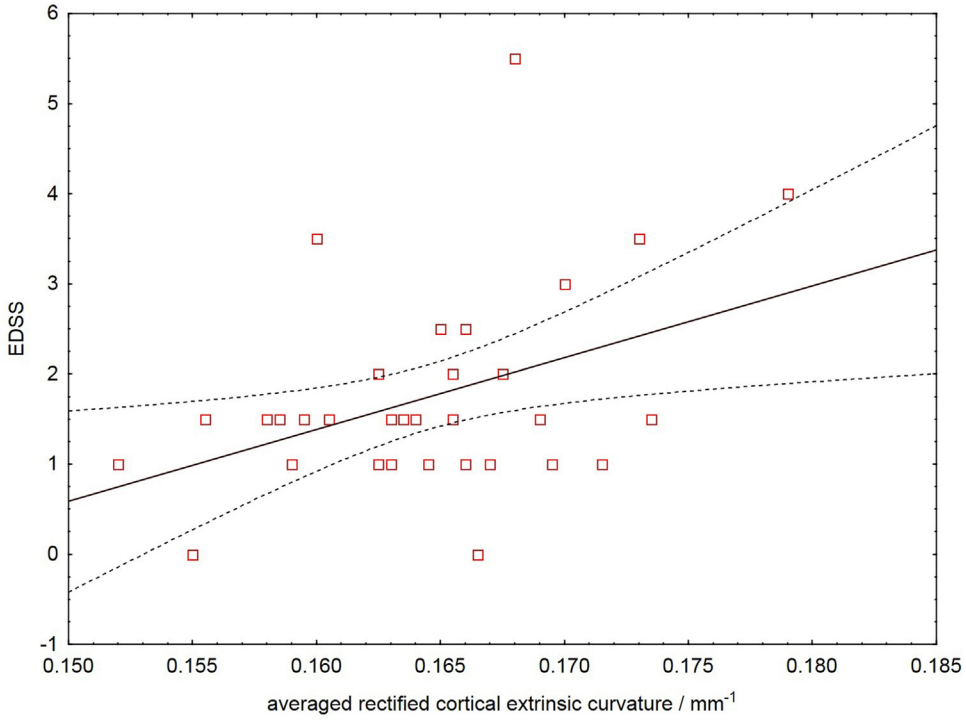

Fig. 13. A more severe EDSS was reflected by an increased cortical curvature ($P < 0.05$).

callosum was selected for the following three reasons. Firstly, axonal damage in conjunction with WM atrophy in the normal-appearing WM of the corpus callosum in postmortem brains of patients with multiple sclerosis was already demonstrated by using quantitative measures of both axonal density and WM atrophy (Evangelou et al., 2000). Secondly, the corpus callosum contains virtually no crossing fibers, so that this ROI seemed particularly qualified to quantify neuronal integrity loss by FA derived from a second-order tensor model (Deppe et al., 2007). Thirdly, a recent study (Mohammadi et al., 2012), showed that volumetric or atrophic effects on the registered diffusion-weighted images are negligible in the corpus callosum if our newly developed rigorous spatial normalization is employed for quantitative FA comparisons. As expected, the FA in the corpus callosum was significantly reduced in the multiple sclerosis group, which can be interpreted as a kind of physical microstructural "thinning-out" effect that leads to a loss of diffusion barriers within the WM. Moreover, within the multiple sclerosis group, the individual FA reduction was significantly correlated with the individual increase in extrinsic curvature; thus, pointing to an association between individual WMV reduction and microstructural WM damage (Fig. 11). These findings of early FA and volume reduction in the corpus callosum are congruent with previous studies showing early degeneration of the corpus callosum over 1 year following the first acute inflammatory episode in patients with multiple sclerosis (Audoin et al., 2007; Ranjeva et al., 2003). A second ROI, encompassing the whole WM, showed very similar effects to those seen in the corpus callosum ROI; therefore, it seems likely that findings in the corpus callosum are representative of the whole WM (Fig. 12).

4.4. Cortical thickness

A low, but significant reduction in cortical thickness was seen in the multiple sclerosis versus the control group (3.6%). This seems relatively small compared with other studies (Calabrese et al., 2007, 2013), but may be explained by the low degree of patient disability in the study presented here. In a histological study, relative neocortical thinning of 10% was reported in patients with multiple sclerosis (Wegner et al., 2006). In contrast to the findings of Sailer et al. (2003), a significant relationship between EDSS and cortical thickness was not established in this study, which may be due to the lack of effect on the cortical GM. However, one patient in our multiple sclerosis group (described as an "outlier" in Fig. 11) differed significantly from the other patients due to their significantly low GMV. Interestingly, the curvature of this patient was less increased than other multiple sclerosis patients, as would be expected when the WM and GM are both atrophic and, therefore, virtually no GM–WM disproportion exists.

4.5. Reliability of cortical curvature estimates

The reliability of the FreeSurfer program for cortical reconstruction, GMV and WMV, and cerebral surface measurements has been assessed previously in a number of studies (Han et al., 2006; Kang et al., 2012b; Keller et al., 2012; Lee et al., 2006; Rosas et al., 2002) and cortical curvature analysis has also been performed on different neurological or psychiatric patients (Ronan et al., 2011b, 2012; Voets et al., 2011). The inter-individual variability of 3.92% (CV%) in whole-brain-averaged absolute extrinsic curvature (see Table 2) was considerably smaller than the variability of the absolute WMV in our control group (13.03%; see Table 1). The low variability in the cortical extrinsic curvature of less than 4% is remarkable, because no normalization to ICV, age, or gender was employed. The cortical extrinsic curvature, therefore, seems to represent a robust and sensitive biomarker for the detection of changes in the GM–WM proportion. A previous study in healthy controls showed mean values of 0.138 mm^{-1} for the whole-brain-averaged cortical curvature and 2.585 mm for average cortical thickness (Kang et al., 2012a), which seem to differ from the values reported in this paper. However, if we assume that both scanners differed in linear length calibration by a factor $f = 2.59$ mm/2.50 mm, their average extrinsic curvature would result in $f \times 0.138\ mm^{-1} = 0.143\ mm^{-1}$ and would thus fit well into the 95% CI of the whole-brain-averaged absolute extrinsic curvature of healthy persons seen in this study. This observation may suggest that even small differences in geometric size calibrations may be important when comparing quantitative results between different scanners or system configurations (see also Han et al., 2006). In Fig. 10, there seems to be a slight age dependent trend of a decreasing

curvature in the control group. This could have occurred by chance (not significant), but would also fit with the finding that the WMV is less affected in "healthy" aging than the GMV (Grossman et al., 2002; Vernooij et al., 2008).

4.6. Consideration of intrinsic curvature

Two types of cortical curvature may be examined in patients with multiple sclerosis. The first type, the *extrinsic* curvature or *mean curvature*, is a curvature that arises from the mechanical folding of the surface, and, as such, is not a property of the surface itself, but rather of how it is embedded in a three-dimensional (3D) space. Extrinsic curvature changes, if a bendable, but non-elastic two-dimensional surface is folded within a 3D space. For example, if we roll up a *flat* piece of paper into a cylinder, the extrinsic curvature c changes, but not the second type, the Gaussian (or *intrinsic*) curvature. In a bendable, but non-elastic, and non-stretchable surface, we cannot change the intrinsic curvature without destroying the surface. For example, it is not possible to fit a piece of paper (Gaussian curvature $= 0.0\ \mathrm{mm}^{-2}$) to the surface of a sphere (Gaussian curvature $= 1 / R^2$) without producing folds and tears (Ronan et al., 2011a).

In the present study, we concentrated on the *extrinsic* or mean curvature. FreeSurfer software also measures Gaussian (or intrinsic) curvature of the cortex. The *intrinsic* curvatures of the patients' cortices were also significantly affected by the atrophy, but showed higher intra-group variability, were less significantly reduced ($t = 4.18$, $P = 0.0001$), and were not so specific than the extrinsic curvatures. Thus, the results about the intrinsic curvature were not reported in detail here.

4.7. Functional relevance of cortical extrinsic curvature increase

Individual disability as expressed by the EDSS was better explained by the extrinsic curvature increase of a patient than by the estimated individual volumetric loss of WM brain parenchyma (ΔWMV) or the WM lesion load (*Part IV-b*). The weak correlation between EDSS and lesion load might be explained by the fact that the (scalar) measure "lesion load" is per se a rather insensitive index because it does not account for the varying functional relevance of different lesion sites. However, it seems to be interesting for further studies to compare how T2w/FLAIR lesions would be correlated to cortical curvature alterations.

4.8. Methodological limitations and future research directions

The results presented here are based only on one single observation per patient, and more assessments over time would be required to define cortical curvature as a longitudinal biomarker of WM atrophy. Furthermore, this study did not examine the prognostic value of the cortical extrinsic curvature for disease progression. The pre-diagnostic levels of WM in these patients are unknown; thus, the degree of atrophy over time and with increasing severity of illness cannot be elucidated. The use of the EDSS as an indicator of disease progression has known limitations due to subjective error and inter-rater variability (Reilmann et al., 2013). Our group of patients with Alzheimer's disease was not age-matched to our control group, as this group served only as a reference for patients with pronounced WM and GM alterations.

This study did not account for the presence of cortical lesions, which potentially could affect the cortex segmentation and reconstruction and could, therefore, also affect local estimates of cortical curvature. However, inspection of the T2-weighted and FLAIR images revealed that relevant lesion load could not be observed in our multiple sclerosis group, thus, the cortical GM was likely intact in these patients. In context with the finding that nearly every patient showed an increased curvature, it is very unlikely, that the increase is relevantly driven by lesions. This hypothesis would be further supported by the fact that the multiple sclerosis patients had only a small reduction in cortical thickness and a cortical GMV in the range of the control group, with the exception of one patient.

This study did not explore any relationship between the curvature alterations and lesion load in multiple sclerosis patients. This might form the basis of future investigations in larger sample groups to explore the effects of specific lesion patterns, like those demonstrated in the study by Giorgio et al., which showed regionally different effects on cortex geometry (Giorgio et al., 2013). It would also be of interest to study WM–GM disproportionality with further quantitative MRI measures, such as myelin water fraction (Kitzler et al., 2012), MRI spectroscopy measures, and histopathology, in order to investigate which predominant factor drives the WM–GM disproportionality and thus the WMV loss. From a translational point of view, it would be also interesting whether cortical curvature correlates better with higher cognitive functions than conventional structural marker like lesion load or volumetric atrophy marker.

5. Conclusion

The present findings provide further evidence that WM atrophy is already present at the very beginning of multiple sclerosis and in every patient suffering with this illness. The increased cortical extrinsic curvature could be used to classify 29/30 patients to the multiple sclerosis group, thus providing a sensitive indicator of WM loss. Overall, the average WM atrophy that we estimated in these 30 patients was 13%, which would be difficult to visualize with conventional MRI methods (2D slices, thickness > 2 mm). However, the specific curvature increase, used as a surrogate measure of WM–GM disproportionality and correlating with FA and EDSS, suggested that WM reduction in this population with multiple sclerosis might be involved in the pathological disease processes that occur independently of GM degeneration. Thus, WM–GM disproportionality and the cortical curvature measurement should be considered as a potential monitoring tool in this devastating, degenerative disorder, and this warrants further assessment in future multiple sclerosis research.

Funding

This work was supported by the Transregional Collaborative Research Center SFB-TR 128 Project B5/B6 and by grants from the German Ministry for Education and Research (BMBF, "German Competence Network Multiple Sclerosis" (KKNMS)).

Acknowledgments

We thank Dr. med. Annette Failing and her team at the radprax Institut für Diagnostik und Forschung, Münster for her kind support and supervision of the MRI examinations.

References

Audoin, B., Ibarrola, D., Malikova, I., Soulier, E., Confort-Gouny, S., Duong, M.V., Reuter, F., Viout, P., Ali-Cherif, A., Cozzone, P.J., Pelletier, J., Ranjeva, J.P., 2007. Onset and underpinnings of white matter atrophy at the very early stage of multiple sclerosis—a two-year longitudinal MRI/MRSI study of corpus callosum. Mult. Scler. 13, 41–51.

Calabrese, M., Atzori, M., Bernardi, V., Morra, A., Romualdi, C., Rinaldi, L., McAuliffe, M.J., Barachino, L., Perini, P., Fischl, B., Battistin, L., Gallo, P., 2007. Cortical atrophy is relevant in multiple sclerosis at clinical onset. J. Neurol. 254, 1212–1220.

Calabrese, M., Favaretto, A., Poretto, V., Romualdi, C., Rinaldi, F., Mattisi, I., Morra, A., Perini, P., Gallo, P., 2013. Low degree of cortical pathology is associated with benign course of multiple sclerosis. Mult. Scler. 19, 904–911.

Chard, D.T., Griffin, C.M., Parker, G.J., Kapoor, R., Thompson, A.J., Miller, D.H., 2002. Brain atrophy in clinically early relapsing–remitting multiple sclerosis. Brain 125, 327–337.

Dale, A.M., Fischl, B., Sereno, M.I., 1999. Cortical surface-based analysis. I. Segmentation and surface reconstruction. NeuroImage 9, 179–194.

De, S.N., Giorgio, A., Battaglini, M., Rovaris, M., Sormani, M.P., Barkhof, F., Korteweg, T., Enzinger, C., Fazekas, F., Calabrese, M., Dinacci, D., Tedeschi, G., Gass, A., Montalban, X., Rovira, A., Thompson, A., Comi, G., Miller, D.H., Filippi, M., 2010. Assessing brain atrophy rates in a large population of untreated multiple sclerosis subtypes. Neurology 74, 1868–1876.

Deppe, M., Duning, T., Mohammadi, S., Schwindt, W., Kugel, H., Knecht, S., Ringelstein, E.B., 2007. Diffusion-tensor imaging at 3 T: detection of white matter alterations in neurological patients on the basis of normal values. Invest. Radiol. 42, 338–345.

Deppe, M., Kellinghaus, C., Duning, T., Moddel, G., Mohammadi, S., Deppe, K., Schiffbauer, H., Kugel, H., Keller, S.S., Ringelstein, E.B., Knecht, S., 2008. Nerve fiber impairment of anterior thalamocortical circuitry in juvenile myoclonic epilepsy. Neurology 71, 1981–1985.

Deppe, M., Müller, D., Kugel, H., Ruck, T., Wiendl, H., Meuth, S.G., 2013. DTI detects water diffusion abnormalities in the thalamus that correlate with an extremity pain episode in a patient with multiple sclerosis. NeuroImage Clin. 2, 258–262.

Duning, T., Kellinghaus, C., Mohammadi, S., Schiffbauer, H., Keller, S., Ringelstein, E.B., Knecht, S., Deppe, M., 2010. Individual white matter fractional anisotropy analysis on patients with MRI negative partial epilepsy. J. Neurol. Neurosurg. Psychiatry 81, 136–139.

Evangelou, N., Esiri, M.M., Smith, S., Palace, J., Matthews, P.M., 2000. Quantitative pathological evidence for axonal loss in normal appearing white matter in multiple sclerosis. Ann. Neurol. 47, 391–395.

Filippi, M., Rocca, M.A., Barkhof, F., Bruck, W., Chen, J.T., Comi, G., DeLuca, G., De, S.N., Erickson, B.J., Evangelou, N., Fazekas, F., Geurts, J.J., Lucchinetti, C., Miller, D.H., Pelletier, D., Popescu, B.F., Lassmann, H., 2012. Association between pathological and MRI findings in multiple sclerosis. Lancet Neurol. 11, 349–360.

Fischl, B., 2012. FreeSurfer. NeuroImage 62, 774–781.

Fischl, B., Dale, A.M., 2000. Measuring the thickness of the human cerebral cortex from magnetic resonance images. Proc. Natl. Acad. Sci. U. S. A. 97, 11050–11055.

Fischl, B., Sereno, M.I., Dale, A.M., 1999. Cortical surface-based analysis. II: inflation, flattening, and a surface-based coordinate system. NeuroImage 9, 195–207.

Giorgio, A., Battaglini, M., Rocca, M.A., De, L.A., Absinta, M., van, S.R., Rovira, A., Tintore, M., Chard, D., Ciccarelli, O., Enzinger, C., Gasperini, C., Frederiksen, J., Filippi, M., Barkhof, F., De, S.N., 2013. Location of brain lesions predicts conversion of clinically isolated syndromes to multiple sclerosis. Neurology 80, 234–241.

Grossman, M., Smith, E.E., Koenig, P., Glosser, G., DeVita, C., Moore, P., McMillan, C., 2002. The neural basis for categorization in semantic memory. NeuroImage 17, 1549–1561.

Han, X., Jovicich, J., Salat, D., van der Kouwe, A., Quinn, B., Czanner, S., Busa, E., Pacheco, J., Albert, M., Killiany, R., Maguire, P., Rosas, D., Makris, N., Dale, A., Dickerson, B., Fischl, B., 2006. Reliability of MRI-derived measurements of human cerebral cortical thickness: the effects of field strength, scanner upgrade and manufacturer. NeuroImage 32, 180–194.

Kang, X., Herron, T.J., Turken, A.U., Woods, D.L., 2012a. Diffusion properties of cortical and pericortical tissue: regional variations, reliability and methodological issues. Magn. Reson. Imaging 30, 1111–1122.

Kang, X., Herron, T.J., Cate, A.D., Yund, E.W., Woods, D.L., 2012b. Hemispherically-unified surface maps of human cerebral cortex: reliability and hemispheric asymmetries. PLoS One 7, e45582.

Keller, S.S., Gerdes, J.S., Mohammadi, S., Kellinghaus, C., Kugel, H., Deppe, K., Ringelstein, E.B., Evers, S., Schwindt, W., Deppe, M., 2012. Volume estimation of the thalamus using Freesurfer and stereology: consistency between methods. Neuroinformatics 10, 341–350.

Keller, S.S., Ahrens, T., Mohammadi, S., Gerdes, J.S., Moddel, G., Kellinghaus, C., Kugel, H., Weber, B., Ringelstein, E.B., Deppe, M., 2013. Voxel-based statistical analysis of fractional anisotropy and mean diffusivity in patients with unilateral temporal lobe epilepsy of unknown cause. J. Neuroimaging 23, 352–359.

Kitzler, H.H., Su, J., Zeineh, M., Harper-Little, C., Leung, A., Kremenchutzky, M., Deoni, S.C., Rutt, B.K., 2012. Deficient MWF mapping in multiple sclerosis using 3D whole-brain multi-component relaxation MRI. NeuroImage 59, 2670–2677.

Kleffner, I., Deppe, M., Mohammadi, S., Schiffbauer, H., Stupp, N., Lohmann, H., Young, P., Ringelstein, E.B., 2008. Diffusion tensor imaging demonstrates fiber impairment in Susac syndrome. Neurology 70, 1867–1869.

Lee, J.K., Lee, J.M., Kim, J.S., Kim, I.Y., Evans, A.C., Kim, S.I., 2006. A novel quantitative cross-validation of different cortical surface reconstruction algorithms using MRI phantom. NeuroImage 31, 572–584.

Miller, D.H., Barkhof, F., Frank, J.A., Parker, G.J., Thompson, A.J., 2002. Measurement of atrophy in multiple sclerosis: pathological basis, methodological aspects and clinical relevance. Brain 125, 1676–1695.

Mohammadi, S., Moller, H.E., Kugel, H., Muller, D.K., Deppe, M., 2010. Correcting eddy current and motion effects by affine whole-brain registrations: evaluation of three-dimensional distortions and comparison with slicewise correction. Magn. Reson. Med. 64, 1047–1056.

Mohammadi, S., Keller, S.S., Glauche, V., Kugel, H., Jansen, A., Hutton, C., Floel, A., Deppe, M., 2012. The influence of spatial registration on detection of cerebral asymmetries using voxel-based statistics of fractional anisotropy images and TBSS. PLoS One 7, e36851.

Pirko, I., Lucchinetti, C.F., Sriram, S., Bakshi, R., 2007. Gray matter involvement in multiple sclerosis. Neurology 68, 634–642.

Polman, C.H., Reingold, S.C., Banwell, B., Clanet, M., Cohen, J.A., Filippi, M., Fujihara, K., Havrdova, E., Hutchinson, M., Kappos, L., Lublin, F.D., Montalban, X., O'Connor, P., Sandberg-Wollheim, M., Thompson, A.J., Waubant, E., Weinshenker, B., Wolinsky, J.S., 2011. Diagnostic criteria for multiple sclerosis: 2010 revisions to the McDonald criteria. Ann. Neurol. 69, 292–302.

Popescu, V., Agosta, F., Hulst, H.E., Sluimer, I.C., Knol, D.L., Sormani, M.P., Enzinger, C., Ropele, S., Alonso, J., Sastre-Garriga, J., Rovira, A., Montalban, X., Bodini, B., Ciccarelli, O., Khaleeli, Z., Chard, D.T., Matthews, L., Palace, J., Giorgio, A., De, S.N., Eisele, P., Gass, A., Polman, C.H., Uitdehaag, B.M., Messina, M.J., Comi, G., Filippi, M., Barkhof, F., Vrenken, H., 2013. Brain atrophy and lesion load predict long term disability in multiple sclerosis. J. Neurol. Neurosurg. Psychiatry.

Ranjeva, J.P., Pelletier, J., Confort-Gouny, S., Ibarrola, D., Audoin, B., Le, F.Y., Viout, P., Cherif, A.A., Cozzone, P.J., 2003. MRI/MRS of corpus callosum in patients with clinically isolated syndrome suggestive of multiple sclerosis. Mult. Scler. 9, 554–565.

Reilmann, R., Holtbernd, F., Bachmann, R., Mohammadi, S., Ringelstein, E.B., Deppe, M., 2013. Grasping multiple sclerosis: do quantitative motor assessments provide a link between structure and function? J. Neurol. 260, 407–414.

Ronan, L., Pienaar, R., Williams, G., Bullmore, E., Crow, T.J., Roberts, N., Jones, P.B., Suckling, J., Fletcher, P.C., 2011a. Intrinsic curvature: a marker of millimeter-scale tangential cortico-cortical connectivity? Int. J. Neural Syst. 21, 351–366.

Ronan, L., Scanlon, C., Murphy, K., Maguire, S., Delanty, N., Doherty, C.P., Fitzsimons, M., 2011b. Cortical curvature analysis in MRI-negative temporal lobe epilepsy: a surrogate marker for malformations of cortical development. Epilepsia 52, 28–34.

Ronan, L., Voets, N.L., Hough, M., Mackay, C., Roberts, N., Suckling, J., Bullmore, E., James, A., Fletcher, P.C., 2012. Consistency and interpretation of changes in millimeter-scale cortical intrinsic curvature across three independent datasets in schizophrenia. NeuroImage 63, 611–621.

Rosas, H.D., Liu, A.K., Hersch, S., Glessner, M., Ferrante, R.J., Salat, D.H., van der Kouwe, A., Jenkins, B.G., Dale, A.M., Fischl, B., 2002. Regional and progressive thinning of the cortical ribbon in Huntington's disease. Neurology 58, 695–701.

Turner, B., Lin, X., Calmon, G., Roberts, N., Blumhardt, L.D., 2003. Cerebral atrophy and disability in relapsing–remitting and secondary progressive multiple sclerosis over four years. Mult. Scler. 9, 21–27.

Vernooij, M.W., de, G.M., van der Lugt, A., Ikram, M.A., Krestin, G.P., Hofman, A., Niessen, W.J., Breteler, M.M., 2008. White matter atrophy and lesion formation explain the loss of structural integrity of white matter in aging. NeuroImage 43, 470–477.

Voets, N.L., Bernhardt, B.C., Kim, H., Yoon, U., Bernasconi, N., 2011. Increased temporolimbic cortical folding complexity in temporal lobe epilepsy. Neurology 76, 138–144.

Wegner, C., Esiri, M.M., Chance, S.A., Palace, J., Matthews, P.M., 2006. Neocortical neuronal, synaptic, and glial loss in multiple sclerosis. Neurology 67, 960–967.

Wersching, H., Duning, T., Lohmann, H., Mohammadi, S., Stehling, C., Fobker, M., Conty, M., Minnerup, J., Ringelstein, E.B., Berger, K., Deppe, M., Knecht, S., 2010. Serum C-reactive protein is linked to cerebral microstructural integrity and cognitive function. Neurology 74, 1022–1029.

Zivadinov, R., 2007. Can imaging techniques measure neuroprotection and remyelination in multiple sclerosis? Neurology 68, S72–S82.

Zivadinov, R., Reder, A.T., Filippi, M., Minagar, A., Stuve, O., Lassmann, H., Racke, M.K., Dwyer, M.G., Frohman, E.M., Khan, O., 2008. Mechanisms of action of disease-modifying agents and brain volume changes in multiple sclerosis. Neurology 71, 136–144.